doi:10.4028/www.scientific.net/MSF.790-791.355

Microstructure evolution in an aluminum cladded sheet during vacuum brazing

Cécile Bernardi[1,2,a], Alain Hazotte[2,b], Nathalie Siredey-Schwaller[2,c], Thierry Mazet[1,d], Jacques Lacaze[3,e]

[1] Fives Cryo, 25 bis rue du Fort - B.P. 87 88194 Golbey Cedex, France

[2] Laboratoire LEM3, Saulcy, Ile du Saulcy F-57045 Metz - Cedex 01, France

[3] CIRIMAT, ENSIACET 4, allée Emile Monso - CS 44362, 31030 Toulouse Cedex 4, France

[a] cecile.bernardi@fivesgroup.com, [b] alain.hazotte@univ-lorraine.fr,

[c] nathalie.siredey@univ-lorraine.fr, [d]thierry.mazet@fivesgroup.com, [e]jacques.lacaze@ensiacet.fr

Keywords : heat exchangers, brazing, aluminum alloys, microstructure

Abstract. Microstructure evolution of a 3003 sheet cladded with 4004 brazing alloy is investigated during slow heating (1K/min) under secondary vacuum up to isothermal brazing temperature (590°C). Optical and scanning microscopies, EDS chemical analysis and EBSD orientation mapping are used. Experimental results are discussed in the light of thermodynamic calculations using Thermo-Calc. Comparisons show good agreement as long as Mg vaporization does not take place.

Introduction

Most of aluminum heat exchangers are brazed in controlled atmosphere brazing (CAB) furnaces, using fluxes to remove the oxide layer on the brazing sheet surface. This study rather focuses on plates and fins heat exchangers brazed under secondary vacuum. They consist of alternative 4004 (clad) / 3003 (core) brazing sheets and 3003 fins. The clad layer melts and flows when the brazing temperature is reached (around 590°C), permitting the junction between the parts to be assembled. Here, magnesium in the 4004 alloy plays the role of the flux [1]. A certain amount of it evaporates above 400°C which disrupts the oxide layer and acts as a getter to prevent from re-oxidation during brazing.

The heating rate of industrial processes is very slow, around 1 K/min and significant long range diffusion takes place, which strongly modifies the microstructure of both alloys before the brazing itself proceeds. This results in deviation from the processing route usually admitted by metallurgists working on aluminum brazing.

The aim of this work is to precisely characterize what happens in 3003/4004 sheets during their slow heating up to brazing temperature.

Materials and methods

Since this work only deals with heating before brazing, tests were carried on a simple brazing sheet. The core is made of a 3003 alloy cladded on both sides with a 125 µm thick 4004 alloy. The total thickness of the sheet is 1 mm. The standard chemical composition of both alloys is listed in Table 1.

The 3003 alloy is characterized by its high level in manganese, while the 4004 is enriched in silicon and magnesium. Si lowers the melting point [2] whilst Mg permits the destruction of the oxide layer.

Table 1. Chemical composition of the two Al-alloys constituting the cladded sheet (wt%).

Alloy	Si	Fe	Cu	Mn	Zn	Mg	Others		Al
							Each	Total	
3003	0.60	0.70	0.05 –0.2	1.0 – 1.5	0.10	0	0.050	0.15	balance
4004	9 –10.5	0.80	0.25	0.10	0.20	1.0-2.0	0.05	0.15	balance

One single cladded sheet was cut into smaller parts on which the tests were made, thus avoiding any ambiguity in terms of chemical composition or thermo-mechanical treatments, which can differ from one supplier to another.

A heating device working in secondary vacuum (10^{-4} mbar) was used to perform heat treatments which consisted of a 1K/min heating to different temperatures followed by a rapid cooling (on the order of 20K/min) to room temperature. The heating rate of 1K/min is closed to the industrial conditions.

Samples were then mounted in a conductive resin and polished. SEM observation and EDS analysis required a mechanical polishing, ending by a ¼ µm diamond suspension, while the final polishing of samples for EBSD analysis was performed with an OPS silica suspension. Optical microscope observations were carried on an Olympus BX61. SEM observation and EDS analysis were made on a Zeiss Supra 40 with a Bruker acquisition system. The interaction volume in chemical analysis is around 2.5 μm^3 for aluminum. EBSD maps were obtained with a Zeiss Supra 40 with a Bruker acquisition system (for the deformed microstructures) or with a Jeol 6490 and Oxford acquisition system.

In addition, thermodynamic calculations were performed using Thermo-Calc software and TCAL-2 database. Amounts and compositions of equilibrium phases were calculated as a function of temperature for both alloys. DICTRA software was also used to predict the diffusion profiles induced by slow heating.

Results and discussion

Initial State. Fig.1.a shows the clad alloy 4004 in its initial state. Three types of particles could be identified by EDS analysis and were found to be pure Si, Mg_2Si and π ($Al_{18}Fe_2Mg_7Si_{10}$) phases.

In the core alloy 3003 (Fig.1.b), two types of particles can be distinguished by their size. The coarser ones, hereafter called precipitates, were analyzed by EDS to be either $Al_6(Mn,Fe)$ or α-Al(Mn,Fe)Si ($Al_{15}Si_2M_4$ where M = Mn+Fe) phases. Accurate EDS or EBSD analyses were not possible on the finer particles, called dispersoids, but it has been showed [3] that they should be α-Al(Mn,Fe)Si phase. Image analysis on the as-received 3003 alloy gave estimate of the volume fractions of dispersoids and precipitates to 1.6 ±0.2 % and 3.6 ±0.4%, respectively.

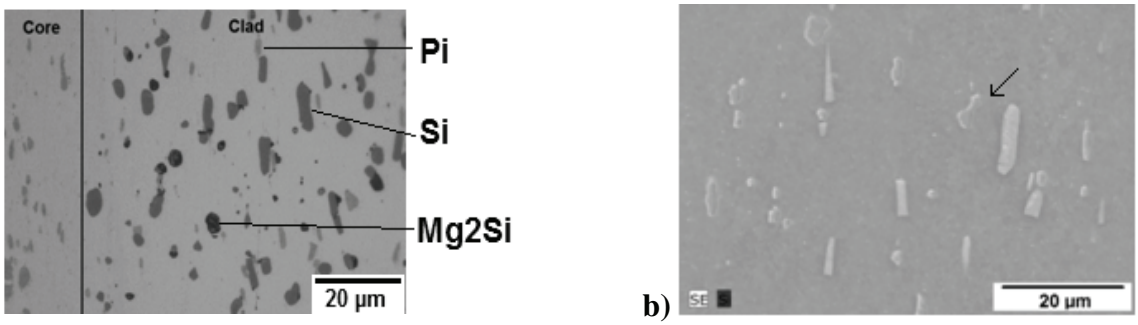

Fig.1. a) Optical micrograph of a cladded sheet at its initial state and b) SEM observation of the core alloy at its initial state coupled with EDS analysis ; Si rich particles (α-Al(Mn,Fe)Si) appear in dark grey (see arrow) whilst the $Al_6(Mn,Fe)$ ones appear in light grey. Rolling direction is vertical.

Fig.2 shows two EBSD maps typical of the laminated material: grains are elongated with numerous internal misorientations. The mean equivalent diameters of 3003 and 4004 grains are around 100 µm and 20 µm, respectively. The deformation cells inside the grains have an estimated diameter of about 1 µm.

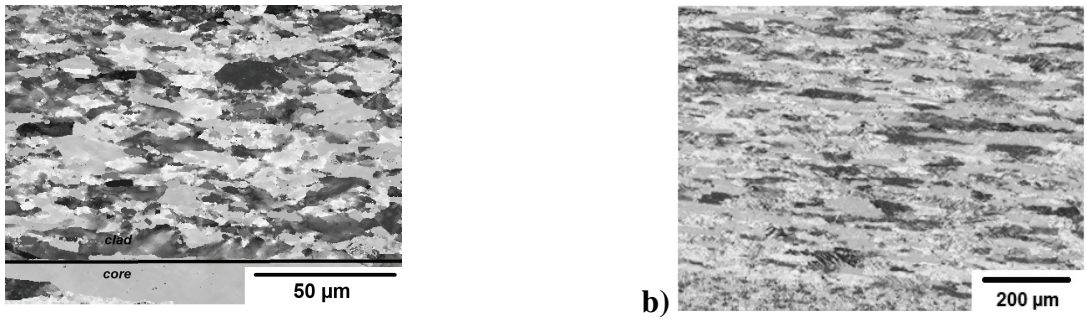

a) b)

Fig.2. EBSD maps showing the grains morphology a) of the clad alloy and b) of the core alloy in their as-received state; rolling direction is horizontal.

Evolution during heating - Thermo-Calc predictions. Equilibrium compositions and proportions of the particles present in both alloys as a function of temperature were calculated by Thermo-Calc. With regard to the very low heating rate used in the present study, it is reasonable to assume that the alloy is close to this equilibrium state for each temperature during heating. However, one should keep in mind that calculations are made for homogeneous alloys and taking neither the vaporization of Mg nor the diffusion of Si into account.

Fig.3 reports the calculated evolution of the weight fractions of phases as a function of temperature for the clad (a) and the core (b) alloys. In the clad alloy (4004), Fig.3.a shows that no major change is expected before 555°C, which is the temperature of formation of the first liquid and relates to a final eutectic reaction involving mainly Si and π phases. That is why most of the following experimental results will concern temperatures higher than 555°C. Above this temperature, the weight fraction of Si and π particles is expected to decrease rapidly as the fraction of liquid increases while $Al_9Fe_2Si_2$ particles should appear at 560°C.

In the core alloy, as shown in Fig.3.b, no drastic change in the total amount of precipitates is expected up to brazing temperature. Indeed, the α-Al(Mn,Fe)Si phase is predicted to slightly grow at the expense of Al_6(Mn,Fe).

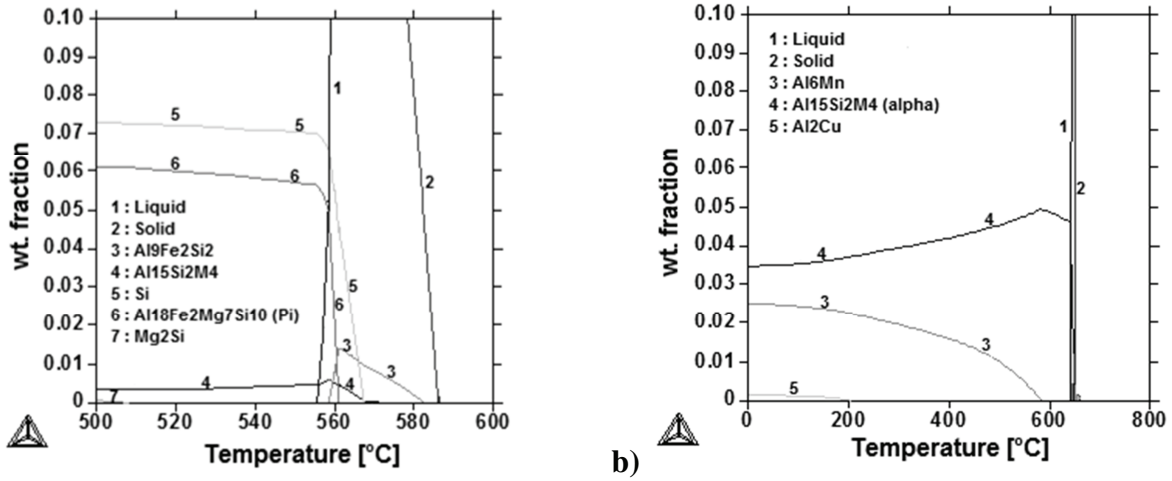

a) b)

Fig.3. Thermo-Calc predictions for the evolution of the particles weight fractions a): in 4004 alloy and b) in 3003 alloy

Evolution during heating - Experimental observations. Fig.4 presents optical micrographs of cladded sheets heated to different temperatures chosen around the ternary eutectic Al-Si-Mg at 555°C and the binary eutectic Al-Si at 577°C. On all the pictures, the clad alloy is on the right side and the core alloy on the left side. These two materials can also be easily distinguished by the quantity and shape of the particles they contain.

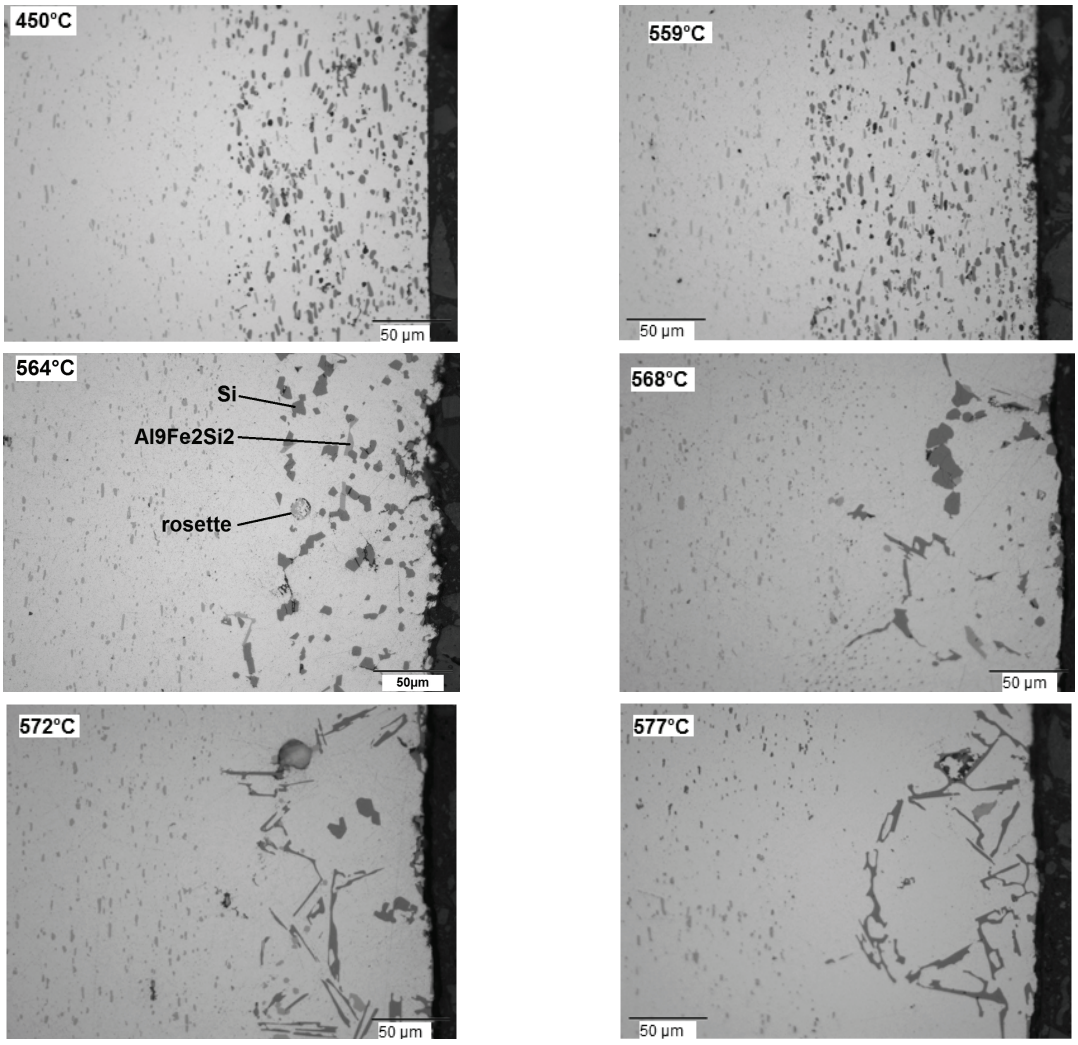

Fig.4. Optical micrographs of a cladded sheet heated to different temperatures. The clad alloy is on the right side and the core alloy on the left side of each micrograph.

Concerning 3003 core alloy, Fig.4 exemplifies no drastic evolution of the morphology of the precipitated phases during heating. EDS analysis also showed no significant change in their composition; they are still $Al_6(Mn,Fe)$ and α-Al(Mn,Fe)Si phases. Volume fractions of dispersoids and precipitates were measured far from the 3003/4004 interface as given in Table 2. It is confirmed that the total amount of precipitates is constant with a trend of coarsening, confirmed by the disappearance of dispersoids. EBSD analysis pointed out that grain recrystallization or recovery takes place very early during heating. As shown in Fig.5, it is still achieved at 428°C, the further evolution being classical grain growth. This recrystallization has a great influence on further brazing during which the liquid clad is in contact with the solid. As mentioned by Schmatz [4], the liquid can penetrate deeper along the grain boundaries. It thus creates an enriched zone in silicon in the core alloy, which could have a strong impact on the corrosion resistance.

In Fig.5 , one also can see that the grains are elongated. This tends to suggest that the major phenomenon taking place for their evolution should be rather recovery than recrystallization. This could be due to the high density of particles existing in the core alloy that prevents recrystallization, as explained by Humphreys [5].

Table 2. Volume fractions of dispersoids and precipitates in the core alloy

	Room T.	425°C	550°C	564°C
Volume fraction of precipitates	3.6±0.9	3.5±0.7	3.3±0.6	3.6±0.7
Volume fraction of dispersoids	1.6±0.2	2.1±0.3	1.1±0.1	0.9±0.2

Fig.5. EBSD maps of the core alloy at two different temperatures

Concerning 4004 clad, Table 3 reports EDS analyses made on the particles detected at different temperatures. As can be seen in Fig.4 and Table 3, no major change is visible until 559°C for the precipitates. This is in accordance with the Thermo-Calc predictions (Fig.3.a), except for the Mg_2Si phase which was present at room temperature and is still observed at 559°C. This may be due to the lack of homogeneity in the alloy and shows that the material was not at equilibrium in its initial state. At a higher temperature, between 559°C and 564°C, liquid is formed in the 4004 alloy, resulting in a drastic change in the microstructure with the melting of the eutectic containing Si and π phases and likely the Mg_2Si phase. In the micrograph for 564°C in Fig.4, it is seen that the Si particles coalesced and new coarse Al_9Fe_2Si particles are formed, which is typical of re-solidification. Rosettes can also be observed [6]. The replacement of Si and π particles by $Al_9Fe_2Si_2$ ones was predicted to start at 560°C by Thermo-Calc (see Fig.3.a), in agreement with what is observed. It has been reported that the liquid resulting from eutectic melting at 555°C does exude on the clad surface [7]. We can assume that the Mg then evaporates, and lets a Si enriched surface. Indeed, on the samples heated to 564°C, numerous and coarse Si particles are observed on the extreme surface of the 4004 alloy.

In addition to Mg evaporation, chemical exchanges occur through the 4004/3003 interface during the whole slow heating process. Firstly, solid state diffusion takes place. In order to reach equilibrium, Si-particles in the clad alloy dissolve and Si diffuses in the core alloy. This has been associated with the creation of a depleted zone free of precipitates between clad and core [1]. This area is visible on Fig.4 at 564°C. Due to the dissolution of core particles, the clad is enriched in Mn. The resulting chemistry variation could explain the presence of Mn in the particles present at 568°C, as seen in Table 3. Indeed, some Mn atoms substituted Fe atoms in the $Al_9Fe_2Si_2$ precipitates, while precipitates with a composition close to α-Al(Mn,Fe)Si appear as previously observed [8].

Table 3. Precipitates present at high temperatures in the 4004 alloy

Sample	Precipitates	Element	Composition found by EDS analysis [at.%]	Stoechiometric compositon [at.%]
559°C	π : $Al_{18}Fe_2Mg_7Si_{10}$	Al Fe Mg Si	56 ± 3 4.5 ± 0.2 16 ± 1.0 24 ± 1.6	49 5,4 19 27
	pure Si	Si Al	78 ± 4,0 21 ± 4,7	100 0
	Mg_2Si	Mg Si Al	21 ± 13 22 ± 3,8 26 ± 14	67 33 0
564°C	$Al_9Fe_2Si_2$	Al Fe Si	68±2.0 13±1.0 18 ± 1.0	69 15 15
	pure Si	Si Al	98 ± 0.7 2,3 ± 0.7	100 0

Sample	Precipitates	Element	Composition found by EDS analysis [at.%]	Stoechiometric compositon [at.%]
568°C	$Al_9Fe_2Si_2$	Al Fe Si Mn	65 ± 1,3 13 ± 0,6 20 ± 1,9 1,7 ± 0,1	69 15 15 0
	pure Si	Si Al	99 ± 0,1 1,4 ± 0,1	100 0
	α-Al(Mn,Fe)Si	Al Fe - Mn Si	72 ± 0,1 11 ± 0,66 - 5,6 ± 0,45 11 ± 0,22	71 Mn + Fe = 19 9,5
573°C	α-Al(Mn,Fe)Si	Al Fe - Mn Si	72 ± 0,10 10,1 ± 0,62 - 6,9 ± 0,48 11 ± 0,13	71 Mn + Fe = 19 9,5
	pure Si	Si Al	98 ± 0,28 2,1 ± 0,28	100 0

EDS analysis put in evidence the diffusion of Si in the core alloy which could be characterized by line countings. Fig. 6 shows that Si diffused over 100 µm in the core alloy. This diffusion depth is in accordance with DICTRA predictions provided that the presence of precipitates is included in the calculations.

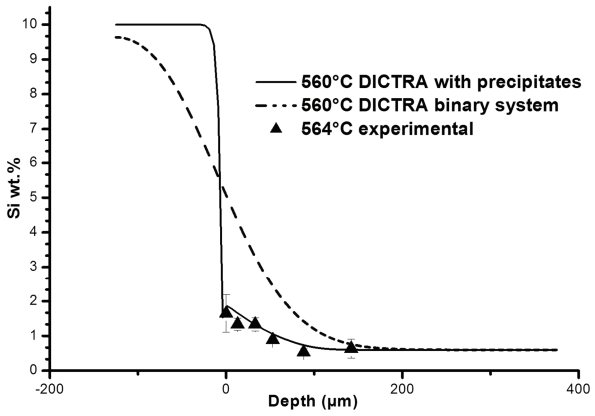

Fig.6. Diffusion of Si from the 4004 alloy to the 3003 alloy; the 0 abscissa is at the interface (end of dispersoids) between clad, on the left part and core, on the right part. Experimental results are compared to a profile obtained by DICTRA for which precipitates containing Si are taken into account. For information, the diffusion profile calculated for the Al-Si binary system is also given.

Conclusions

The evolution of the brazing sheet material during heating before reaching the brazing temperature has been studied and phenomena that have direct consequences on the brazing process have been observed. Below 564°C, the evolution of the microstructure is well described by Thermo-Calc, while at higher temperatures diffusion of Si and vaporization of Mg take place, strongly modifying the material structure. Both calculations and experiments show that melting of the clad begins before the brazing temperature is reached. Due to this early melting, a zone enriched in Si appears at the surface of the clad alloy, and a zone free of precipitates is formed at the interface between clad and core alloys.

The diffusion of Si within the core material during the heating process takes place over an important depth (100 µm) that is correctly predicted by DICTRA if the presence of precipitates in the core alloy is taken into account.

Finally, recovery and/or recrystallization is observed in the core alloy, which is expected to have a beneficial influence on brazing because it creates coarse grains.

References

[1] J.R. Terrill, C. N. Cochran, J.J. Strokes, W.E. Haupin, Understanding the Mechanisms of Aluminum Brazing can improve results in production operations, Weld. J. (1971) 833-839.

[2] J.C. Ambrose, M. G. Nicholas, Alloys for Vacuum Brazing Aluminum, One-Day Seminar “The Metallurgy of Soldered and Brazed Joints” (1986) 34-38.

[3] G.J. Marshall, R. K. Bolingbroke, A. Gray, Microstructural Control in an Aluminum Core Alloy for Brazing Sheet Applications, Metall. Trans. A 24A (1993) 1935-1942.

[4] D.J. Schmatz, Grain boundary Penetration During Brazing of Aluminum, Wel. Res. S. (1983) 267-271-s

[5] F.J. Humphreys and M. Hatherly, Recrystallization and Related Annealing Phenomena, Pergamon, 2000.

[6] S. Ahrweiler, L. Ratke, J. Lacaze, Microsegregation and microstructural feature of directionally solidified AlSi and AlSiMg alloys, Adv. Eng. Mater. 5 (2003) 17-23

[7] W.A. Anderson, Metallurgical Studies of the Vacuum Brazing of Aluminum, Weld. Res. S. (1977) 314-318-s.

[8] J. Lacaze, S. Tierce, M.-C. Lafont, Y. Thebault, N. Pébère, G. Mankowski, C. Blanc, H. Robidou, D. Vaumousse, D. Daloz, Study of the microstructure resulting from brazed aluminium materials used in heat exchangers, Mater. Sci. and Eng.A, 413-414 (2005) 317-321.